Modelling of Polymeric Fluid Flow Taking into Account the Electromagnetic Impacts and the Heat Dissipation*

ALEXANDER BLOKHIN[1], EKATERINA KRUGLOVA[2,3], BORIS SEMISALOV[2,3]

[1] Sobolev Institute of Mathematics SB RAS, 630090 Novosibirsk, Russia
[2] Novosibirsk State University, 630090 Novosibirsk, Russia
[3] Institute of Computational Technologies SB RAS, 630090 Novosibirsk, Russia
blokhin@math.nsc.ru, sl2857@mail.ru, ViBiS@ngs.ru

Abstract: A new mathematical model describing non-isothermal flow of incompressible viscoelastic polymeric liquid between two coaxial cylinders has been developed on the basis of the mesoscopic approach to polymer dynamics. This model is a system of non-linear PDEs taking into account the electromagnetic impacts and the dissipation of heat. Integral expression for determining the velocity of flow is derived and boundary value problem for temperature is posed. For calculating the velocity and temperature profiles Chebyshev approximations were used and the pseudospectral numerical algorithm was constructed. The stationary numerical solutions are obtained for wide range of values of physical parameters and for record-low values of the radius r_0 of the inner cylinder.

Keywords: polymer dynamics, mesoscopic approach, magnetohydrodynamics, heat dissipation, coaxial cylinders, singularly perturbed problem, pseudospectral method, Chebyshev polynomials.

1 Introduction

In the present times the additive manufacturing (3D printing) using polymer materials is one of the most demanded and fast-growing industries. This work is devoted to the reliable mathematical modelling and accurate numerical simulation of flows of polymeric solutions and melts through the channels of printing machines on the basis of *mesoscopic theory of polymer dynamics* [1,2]. It is the natural extension of the series of works [1–7], where the development and validation of modified *rheological Pokrovskii–Vinogradov model* that takes into account thermomechanical and electromagnetic properties of polymeric liquids were done; the derivation of resolving systems of quasi-linear PDEs describing the flows through channels of different forms that are qualitatively similar to the classical Poiseuille and Couette ones was given; and the methods and algorithms for solving these PDEs were designed.

In [7] the problem of non-isothermal *flows of polymeric liquid between two coaxial cylinders* has been posed and solved numerically for various values of physical and geometrical parameters. In this work we consider the similar problem, but here a new way of deriving the resolving equations is used, and that is the main novelty, we supplement a model with the equations for the components of magnetic field intensity and with the heat-conducting equation having the specific heat dissipation term. This leads to significant changes in the velocity profiles and other characteristics of the flow and allows for increasing its physical reliability by taking into account a number of effects inspired by the dissipation of heat and the magnetic impacts.

For solving the stationary boundary-value problem describing the non-isothermal flow of polymeric liquid between to coaxial cylinders the pseudospectral algorithm developed in [8] and based on Chebyshev approximations has been used. It is worth noting that the asymptotic of error of Chebyshev approximations and of the applied algorithm strictly corresponds to that of the best polynomial approximations [9,10] (in Russian literature this property is known as "*the absence of saturation of the algorithm*", see [11]). This enabled us to derive the reliable and accurate error estimates for approximate solutions of the simplified problem in [12]. In the more complex model considered in this work the application of such algorithm also gave us the opportunity to obtain the solution for singularly perturbed problem with extremely small values of the radius of inner cylinder.

*Two authors of the paper, Boris Semisalov and Ekaterina Kruglova, would like to acknowledge Russian Science Foundation (project No. 17-71-10135) for financial support

2 Preliminary information

2.1 Governing equations of magnetohydrodynamics

Following the results of the books [13–17] and of the papers [4,18] let us write governing system of equations of a new mathematical model describing *magnetohydrodynamical non-isothermal flows of an incompressible polymeric liquid*. These equations written in the dimensionless form in the cylindrical coordinate system are as follows:

$$\operatorname{div}\vec{u} = \frac{\partial u}{\partial r} + \frac{1}{r}\frac{\partial v}{\partial \varphi} + \frac{\partial w}{\partial z} + \frac{u}{r} = 0, \tag{1}$$

$$\operatorname{div}\vec{H} = \frac{1}{r}\frac{\partial (rL)}{\partial r} + \frac{1}{r}\frac{\partial M}{\partial \varphi} + \frac{\partial N}{\partial z} = 0, \tag{2}$$

$$\frac{\partial u}{\partial t} + \frac{\partial P}{\partial r} = \frac{1}{\mathrm{Re}}\left\{\frac{\partial (Ya_{rr})}{\partial r} + \frac{1}{r}\frac{\partial (Ya_{r\varphi})}{\partial r} + \frac{\partial (Ya_{rz})}{\partial z} + \frac{a_{rr} - a_{\varphi\varphi}}{r}Y\right\} + \frac{v^2}{r} + \sigma_m\left\{L\frac{\partial L}{\partial r} + \frac{M}{r}\frac{\partial L}{\partial \varphi} + N\frac{\partial L}{\partial z} - \frac{M^2}{r}\right\}, \tag{3}$$

$$\frac{dv}{dt} + \frac{1}{r}\frac{\partial P}{\partial \varphi} = \frac{1}{\mathrm{Re}}\left\{\frac{\partial (Ya_{r\varphi})}{\partial r} + \frac{1}{r}\frac{\partial (Ya_{\varphi\varphi})}{\partial \varphi} + \frac{\partial (Ya_{\varphi z})}{\partial z} + \frac{2}{r}Ya_{r\varphi}\right\} - \frac{uv}{r} + \sigma_m\left\{L\frac{\partial M}{\partial r} + \frac{M}{r}\frac{\partial M}{\partial \varphi} + N\frac{\partial M}{\partial z} + \frac{LM}{r}\right\}, \tag{4}$$

$$\frac{dw}{dt} + \frac{\partial P}{\partial z} = \frac{1}{\mathrm{Re}}\left\{\frac{\partial (Ya_{rz})}{\partial r} + \frac{1}{r}\frac{\partial (Ya_{\varphi z})}{\partial \varphi} + \frac{\partial (Ya_{zz})}{\partial z} + \frac{1}{r}Ya_{rz}\right\} + \sigma_m\left\{L\frac{\partial N}{\partial r} + \frac{M}{r}\frac{\partial N}{\partial \varphi} + N\frac{\partial N}{\partial z}\right\} + \mathrm{Ga}(Y-1), \tag{5}$$

$$\frac{dL}{dt} - \left\{L\frac{\partial u}{\partial r} + \frac{M}{r}\frac{\partial u}{\partial \varphi} + N\frac{\partial u}{\partial z}\right\} - b_m\left\{\Delta_{r,\varphi,z}L - \frac{2}{r^2}\frac{\partial M}{\partial \varphi} - \frac{L}{r^2}\right\} = 0, \tag{6}$$

$$\frac{dM}{dt} + \frac{vL}{r} - \left\{L\frac{\partial v}{\partial r} + \frac{M}{r}\frac{\partial v}{\partial \varphi} + N\frac{\partial v}{\partial z} + \frac{Mu}{r}\right\} - b_m\left\{\Delta_{r,\varphi,z}M + \frac{2}{r^2}\frac{\partial L}{\partial \varphi} - \frac{M}{r^2}\right\} = 0, \tag{7}$$

$$\frac{dN}{dt} - \left\{L\frac{\partial w}{\partial r} + \frac{M}{r}\frac{\partial w}{\partial \varphi} + N\frac{\partial w}{\partial z}\right\} - b_m\Delta_{r,\varphi,z}N = 0, \tag{8}$$

$$\frac{da_{rr}}{dt} - 2\left\{A_r\frac{\partial u}{\partial r} + \frac{a_{r\varphi}}{r}\frac{\partial u}{\partial \varphi} + a_{rz}\frac{\partial u}{\partial z}\right\} + \mathfrak{L}_{rr} = 0, \tag{9}$$

$$\frac{da_{\varphi\varphi}}{dt} + 2\left(\frac{v}{r} - \frac{\partial v}{\partial r}\right)a_{r\varphi} - 2\left\{\frac{1}{r}(u + \frac{\partial v}{\partial \varphi})A_\varphi + a_{\varphi z}\frac{\partial v}{\partial z}\right\} + \mathfrak{L}_{\varphi\varphi} = 0, \tag{10}$$

$$\frac{da_{zz}}{dt} - 2\left\{a_{rz}\frac{\partial w}{\partial r} + \frac{a_{\varphi z}}{r}\frac{\partial w}{\partial \varphi} + A_z\frac{\partial u}{\partial z}\right\} + \mathfrak{L}_{zz} = 0, \tag{11}$$

$$\frac{da_{r\varphi}}{dt} + \left(\frac{v}{r} - \frac{\partial v}{\partial r}\right)A_r + \left\{a_{r\varphi}\frac{\partial w}{\partial z} - a_{rz}\frac{\partial v}{\partial z} - \frac{A_\varphi}{r}\frac{\partial u}{\partial \varphi} - a_{\varphi z}\frac{\partial u}{\partial z}\right\} + \mathfrak{L}_{r\varphi} = 0, \tag{12}$$

$$\frac{da_{rz}}{dt} - a_{rz}\left(\frac{\partial u}{\partial r} + \frac{\partial w}{\partial z}\right) - \left\{A_r\frac{\partial w}{\partial r} + \frac{a_{r\varphi}}{r}\frac{\partial w}{\partial \varphi} + \frac{a_{\varphi z}}{r}\frac{\partial u}{\partial \varphi} + A_z\frac{\partial u}{\partial z}\right\} + \mathfrak{L}_{rz} = 0, \tag{13}$$

$$\frac{da_{\varphi z}}{dt} + \left(\frac{v}{r} - \frac{\partial v}{\partial r}\right)a_{rz} - \left\{a_{\varphi z}\frac{\partial u}{\partial r} + A_z\frac{\partial v}{\partial z} + a_{r\varphi}\frac{\partial w}{\partial r} + \frac{A_\varphi}{r}\frac{\partial w}{\partial \varphi}\right\} + \mathfrak{L}_{\varphi z} = 0, \tag{14}$$

$$\frac{dY}{dt} = \frac{1}{\mathrm{Pr}}\Delta_{r,\varphi,z}Y + \frac{A}{\mathrm{Pr}}Y\Phi + \frac{A_m}{\mathrm{Pr}}\Phi_m. \tag{15}$$

Here t is the time variable, u, v, w are the components of the velocity vector $\vec{u}$, L, M, N are the components of *the vector of magnetic field intensity* $\vec{H}$ in the cylindrical coordinate system;

$P = p + \sigma_m \frac{\| \vec{H} \|^2}{2}$, p is the pressure, $\| \vec{H} \|^2 = (\vec{H}, \vec{H})$;

$a_{rr}, ..., a_{\varphi z}$ are the components of *the symmetric tensor of anisotropy* Π having the second rank;

$$\mathfrak{L}_{rr} = (K_I a_{rr} + \beta \| \vec{a}_r \|^2) / \bar{\tau}_0(Y), \quad \vec{a}_r = (a_{rr}, a_{r\varphi}, a_{rz}),$$

$$\mathfrak{L}_{\varphi\varphi} = (K_I a_{\varphi\varphi} + \beta \| \vec{a}_\varphi \|^2) / \bar{\tau}_0(Y), \quad \vec{a}_\varphi = (a_{r\varphi}, a_{\varphi\varphi}, a_{\varphi z}),$$

$$\mathfrak{L}_{zz} = (K_I a_{zz} + \beta \| \vec{a}_z \|^2) / \bar{\tau}_0(Y), \quad \vec{a}_z = (a_{rz}, a_{\varphi z}, a_{zz}),$$

$$\mathfrak{L}_{r\varphi} = (K_I a_{r\varphi} + \beta(\vec{a}_r, \vec{a}_\varphi)) / \bar{\tau}_0(Y),$$
$$\mathfrak{L}_{rz} = (K_I a_{rz} + \beta(\vec{a}_r, \vec{a}_z)) / \bar{\tau}_0(Y),$$
$$\mathfrak{L}_{\varphi z} = (K_I a_{\varphi z} + \beta(\vec{a}_\varphi, \vec{a}_z)) / \bar{\tau}_0(Y),$$

$K_I = W^{-1} + \frac{\bar{k}}{3} I$, $\bar{k} = k - \beta$, $I = a_{rr} + a_{\varphi\varphi} + a_{zz}$ is the first invariant of the tensor of anisotropy Π;

k and β $(0 < \beta < 1)$ are *the phenomenological parameters* of the rheological Pokrovsky–Vinogradov model (see [4–7,13]);

$A_r = a_{rr} + W^{-1}$, $A_\varphi = a_{\varphi\varphi} + W^{-1}$, $A_z = a_{zz} + W^{-1}$;

$Y = T / T_0$, T is the temperature, $T_0 = 300^\circ$K is the temperature of surrounding environment;

$\bar{\tau}_0(Y) = \frac{J(Y)}{Y}$, $J(Y) = \exp\left(-\bar{E}_A \frac{Y-1}{Y} \right)$;

Φ and Φ_m are the dissipative functions (see Remark 1);

$$\Delta_{r,\varphi,z} = \frac{\partial^2}{\partial r^2} + \frac{1}{r^2}\frac{\partial^2}{\partial \varphi^2} + \frac{\partial^2}{\partial z^2} + \frac{1}{r}\frac{\partial}{\partial r},$$

$$\frac{d}{dt} = \frac{\partial}{\partial t} + u\frac{\partial}{\partial r} + \frac{v}{r}\frac{\partial}{\partial \varphi} + w\frac{\partial}{\partial z};$$

$\mathrm{Ga} = \frac{\mathrm{Ra}}{\mathrm{Pr}}$ is the Grashof number, $\bar{E}_A = \frac{E_A}{T_0}$; the constants Ra (Rayleigh number), Pr (Prandtl number), Re (Reynolds number), E_A (activation energy) are described in [4, 7] in detail;

W is the Weissenberg number;

A, A_m are the dissipative coefficients;

$\sigma_m = \frac{\mu_0 H_0^2}{\rho u_H^2}$ is the magnetic pressure coefficient,

$b_m = \frac{1}{\mathrm{Re}_m}, \mathrm{Re}_m = \sigma_m \mu_0 u_H l$ is the magnetic Reynolds number, μ_0 is the magnetic permeability of vacuum, σ_m is the electrical conductivity of the medium.

The variables t, r, z, u, v, w, p, L, M, N, $a_{rr}, ..., a_{\varphi z}$ in the system (1)–(15) are related to l/u_H, l, u_H, ρu_H^2, H_0, $W/3$, where l is the characteristic length, u_H is the characteristic velocity, ρ=(const) is the density of medium, H_0 is the characteristic value of magnetic field intensity.

Magnetohydrodynamic equations (1)–(15) have been derived using the *Maxwell's equations* (see [14,16]), where the *vector of magnetic induction* $\vec{B}$ was taken as follows:

$$\vec{B} = \mu_0 \vec{H}.$$

In fact a more general relation is valid (see [20,21]):

$$\vec{B} = \mu\mu_0 \vec{H} = (1 + \chi)\mu_0 \vec{H}, \qquad (16)$$

where μ is the magnetic permeability, χ is the magnetic susceptibility, and besides

$$\chi = \chi_0 / Y, \qquad (17)$$

where χ_0 is the magnetic susceptibility for $T = T_0 (= 300^\circ K)$.

Remark 1. The equation (15) differs from the temperature equation in [4,7,18] by the presence of summands with dissipative functions Φ, Φ_m. Following [19] we specify the functions Φ, Φ_m in the form:

$$\Phi = \Pi : \nabla\vec{u} = \sum_{i,j=1}^{3} a_{ij}\frac{\partial u_j}{\partial x_i} = \left\{ a_{11}\frac{\partial u_1}{\partial x_1} + \right.$$
$$+\left(\frac{\partial u_1}{\partial x_2}+\frac{\partial u_2}{\partial x_1}\right)a_{12}+\left(\frac{\partial u_1}{\partial x_3}+\frac{\partial u_3}{\partial x_1}\right)a_{13}+ \qquad (18)$$
$$\left. +a_{22}\frac{\partial u_2}{\partial x_2}+\left(\frac{\partial u_2}{\partial x_3}+\frac{\partial u_3}{\partial x_2}\right)a_{23}+a_{33}\frac{\partial u_3}{\partial x_3}\right\},$$

$$\Phi_m = \sigma_m\Pi_m : \nabla\vec{u} = \sigma_m\sum_{i,j=1}^{3} L_iL_j\frac{\partial u_j}{\partial x_i} =$$
$$\sigma_m\left\{ L_1^2\frac{\partial u_1}{\partial x_1}+L_2^2\frac{\partial u_2}{\partial x_2}+L_3^2\frac{\partial u_3}{\partial x_3}+\right.$$
$$\left(\frac{\partial u_1}{\partial x_2}+\frac{\partial u_2}{\partial x_1}\right)L_1L_2+\left(\frac{\partial u_1}{\partial x_3}+\frac{\partial u_3}{\partial x_1}\right)L_1L_3+ \qquad (19)$$
$$\left. +\left(\frac{\partial u_2}{\partial x_3}+\frac{\partial u_3}{\partial x_2}\right)L_2L_3\right\}.$$

Here $a_{11},...,a_{33}$ are the components of the tensor of anisotropy written in the Cartesian coordinate system $x_1(=x)$, $x_2(=y)$, $x_3(=z)$; u_1, u_2, $u_3(=w)$ and L_1, L_2, $L_3=(N)$ are the components of the velocity vector $\vec{u}$ and of the vector of magnetic field intensity $\vec{H}$ written in the Cartesian coordinate system x, y, z; $\Pi_m = (L_iL_j), i, j = 1,2,3.$

In Figure 1 the vector $\vec{g} = -g(0,0,1)^T$, where g is the gravitational acceleration. This quantity enters the definition of the Rayleigh and Grashof numbers that specify the convective flows of liquid in gravity.

Below we shall seek the stationary solutions of the system (1)–(15) describing the flows of incompressible polymeric liquid between two *coaxial cylinders*. The outer cylinder has a wall of finite thickness Rh, and the inner one is a heating element (see Figure 1). The characteristic length l has been taken equal to R, therefore the dimensionless thickness of the outer cylinder is h. The dimensionless radius of the heating element was denoted by $r_0 : 0 < r_0 < 1$. The relations (1)–(15) should be supplemented with the boundary conditions:

$$r = r_0 : \vec{u} = 0, Y = Y_H, \quad r = 1 : \vec{u} = 0, Y = 1. \quad (20)$$

The quantity Y_H and other boundary conditions are discussed below. Here we only note that $Y_H > 1$ is the heating from inside (in this case we take $\mathrm{Ga}\cdot\mathrm{Re} = 1$) and $Y_H < 1$ is the heating from outside of the channel (in this case we take $\mathrm{Ga}\cdot\mathrm{Re} = -1$). In Figure 1 the magnetic field is also shown. The characteristic value of the magnetic field intensity was set equal to the value of certain outer magnetic field intensity $H_0 = \hat{N}_0$, therefore the dimensionless $\hat{N}_0 = 1$. Notations '0' and '1' refer to the domains: and respectively, 'H' refers to the heating element. We assume, that in the domains '0' and '1' the temperature T is constant and equals to T_0 ($T_0 = 300^\circ K$).

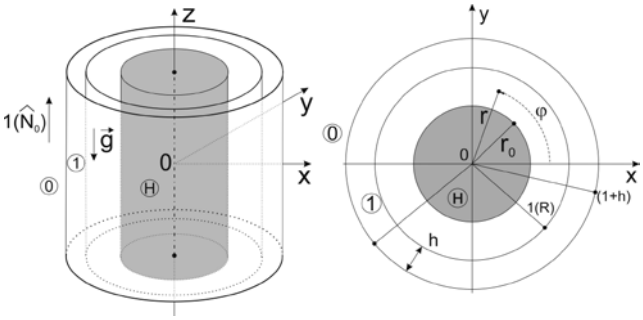

Fig.1. Channel formed by two coaxial cylinders: the channel in Cartesian coordinates x, y, z and the cross-section of channel in polar coordinates.

2.2 Description of the heating element

We assume the heating element 'H' to be a long straight-line cylinder of the radius $r_0 : 0 < r_0 < 1$ manufactured of *paramagnetic material* (for example, aluminum or tungsten) with magnetic susceptibility $\chi_{OH} > 0$ (the value of χ_{OH} is taken from reference tables, [20]). The current-conducting wire is wound on the heating element and there are n turns per each meter (see Figure 2). An electric current is passed through the winding, the current strength is $\hat{I}_H$. Following [20–22], let us express the component of magnetic field intensity $\hat{N}_H$ in the cylinder:

$$\hat{N}_H = n\hat{I}_H \left(\frac{\mathrm{A}}{\mathrm{m}}\right), \qquad (21)$$

therefore the dimensionless magnetic field intensity $\hat{N}_H$ is the following :

$$\hat{N}_H = \frac{n\hat{I}_H}{\hat{N}_0}. \qquad (22)$$

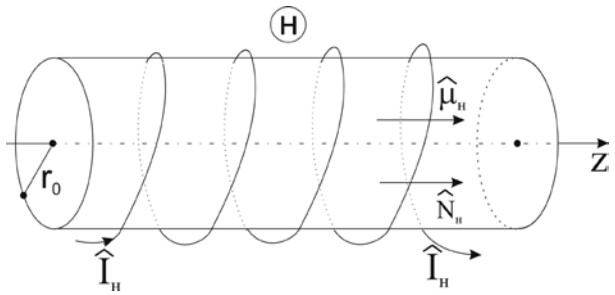

Fig.2. Sketch of the heating element

In (21) the value of $\hat{N}_H$ is given in the SI (see [20]) system and the corresponding dimension is given in brackets. We assume the material of the heating element to be the ideal paramagnetic, therefore the Curie's law is satisfied, [20–23]:

$$\vec{\mathfrak{m}}_H = \chi_H \hat{N}_H, \tag{23}$$

here $\vec{\mathfrak{m}}_H$ is the magnetization. Taking into account (17), (21), (23) we obtain Y_H on the boundary of heating element

$$Y_H = \frac{\chi_{OH}\ \hat{N}_H}{\vec{\mathfrak{m}}_H} = \chi_{OH}\ \frac{n\hat{I}_H}{\vec{\mathfrak{m}}_H} = \chi_{OH}\ \frac{a}{b}, \tag{24}$$

where $a = \dfrac{n\hat{I}_H}{\hat{N}_0}$, $b = \dfrac{\vec{\mathfrak{m}}_H}{\hat{N}_0}$ and the value of χ_{OH} can be taken from the reference tables [20].

It is well-known (see for instance [21, 22]), that a surface current appears on the surface of the paramagnetic whose linear density is equal to $\vec{\mathfrak{m}}_H$. Thus, in (1)–(15) $L = N = 0$ and on the boundary $r = r_0$ this system should be supplemented with one more condition (see (22), (24)):

$$N = (\hat{N}_H + \vec{\mathfrak{m}}_H)/\hat{N}_0 = \frac{n\hat{I}_H}{\hat{N}_0}\mu_H, \tag{25}$$

where $\mu_H = (1 + \chi_{OH}/Y_H)$, see (17).

3 Stationary system of resolving equations

Here we derive a system of non-linear equations describing the flows between two co-axial cylinders that are qualitatively similar to classical Poiseuille ones. To this end let

$$\begin{aligned} &\vec{U}(t,r,\varphi,z) = \hat{\mathbf{U}}(r), \\ &P(t,r,\varphi,z) = \hat{P}(r) - \hat{A}z, \end{aligned} \tag{26}$$

where:

$$\vec{U} = (u, v, w, L, M, N, a_{rr}, ..., a_{\varphi z}, Y)^T,$$

$$\hat{\mathbf{U}} = (0, 0, \hat{w}(r), 0, 0, \hat{N}(r), \hat{a}_{rr}(r), ..., \hat{a}_{\varphi z}(r), \hat{Y}(r))^T,$$

$$\hat{P}(r) = \hat{p}(r) + \sigma_m \frac{\hat{N}^2(r)}{2},$$

$\hat{A} > 0$ is the dimensionless constant pressure drop along Oz axis.

For calculating the functions $\hat{w}(r)$, $\hat{N}(r)$, $\hat{a}_{rr}(r), ..., \hat{a}_{\varphi z}(r)$, $\hat{Y}(r)$, $\hat{P}(r)$ the relations (3)–(5), (9)–(15), (8) can be correspondingly rewritten as follows:

$$\left(\hat{P} - \frac{\hat{Y}\hat{a}_{rr}}{\mathrm{Re}}\right)_\sigma = \frac{\xi_0}{\mathrm{Re}}(\hat{a}_{\varphi\varphi} - \hat{a}_{rr})\hat{Y},\ (\cdot)_\sigma = \frac{d}{d\sigma}, \tag{27}$$

$$\hat{Y}\hat{a}_{r\varphi} = e^{2\xi_0\sigma}\mathbb{C}_{r\varphi}, \tag{28}$$

$$\begin{aligned} \hat{Y}\hat{a}_{rz} = e^{\xi_0\sigma}\Big[\overline{\mathbb{C}} - \tilde{D}e^{-2\xi_0\sigma} + \\ + \mathrm{Ga}^* \xi_0 \int_0^\sigma e^{-2\xi_0\lambda}\hat{Y}d\lambda\Big] = e^{\xi_0\sigma}\tilde{Z}, \end{aligned} \tag{29}$$

$$K_{\hat{I}}\hat{a}_{rr} + \beta \| \hat{\vec{a}}_r \|^2 = 0, \tag{30}$$

$$K_{\hat{I}}\hat{a}_{\varphi\varphi} + \beta \| \hat{\vec{a}}_\varphi \|^2 = 0, \tag{31}$$

$$K_{\hat{I}}\hat{a}_{zz} + \beta \| \hat{\vec{a}}_z \|^2 + 2\hat{a}_{rz}\hat{\nu}\hat{w}_\sigma J(\hat{Y})/\hat{Y} = 0, \tag{32}$$

$$K_{\hat{I}}\hat{a}_{r\varphi} + \beta(\hat{\vec{a}}_r, \hat{\vec{a}}_\varphi) = 0, \tag{33}$$

$$K_{\hat{I}}\hat{a}_{rz} + \beta(\hat{\vec{a}}_r, \hat{\vec{a}}_z) + \hat{A}_r\hat{\nu}\hat{w}_\sigma J(\hat{Y})/\hat{Y} = 0, \tag{34}$$

$$K_{\hat{I}}\hat{a}_{\varphi z} + \beta(\hat{\vec{a}}_\varphi, \hat{\vec{a}}_z) + \hat{a}_{r\varphi}\hat{\nu}\hat{w}_\sigma J(\hat{Y})/\hat{Y} = 0, \tag{35}$$

$$\hat{Y}_{\sigma\sigma} - \frac{A}{\hat{\nu}}\hat{Y}\hat{a}_{rz}\hat{w}_\sigma = 0, \tag{36}$$

$$\hat{N}_{\sigma\sigma} = 0, \quad \hat{N} = \mathbb{C}_1\sigma + \mathbb{C}_2. \tag{37}$$

Here $\sigma = \xi/\xi_0$, $r = e^{-\xi}$, $\xi_0 = -\ln r_0$, $0 \le \sigma \le 1$, $\hat{\nu} = e^{\xi_0\sigma}/\xi_0$, $\hat{w}_\sigma = \dfrac{d\hat{w}}{d\sigma} = -\dfrac{1}{\hat{\nu}}\dfrac{d\hat{w}}{dr}$,

$$\tilde{Z} = \overline{\mathbb{C}} - \tilde{D}e^{-2\xi_0\sigma} + \mathrm{Ga}^*\xi_0\int_0^\sigma e^{-2\xi_0\lambda}\hat{Y}d\lambda,$$

$$\overline{\mathbb{C}} = \hat{a}_{rz}\,|_{\sigma=0} + \tilde{D}, \quad \tilde{D} = \frac{\hat{D} - \mathrm{Ga}^*}{2}, \quad \mathrm{Ga}^* = \mathrm{GaRe},$$

$\hat{D} = \hat{A}\mathrm{Re}$, $\mathbb{C}_{r\varphi}$, $\mathbb{C}_1$, $\mathbb{C}_2$ are the certain constants,

$$\hat{A}_r = \hat{a}_{rr} + W^{-1}, K_{\hat{I}} = W^{-1} + \frac{\overline{k}}{3}\hat{I},$$

$$\hat{I} = \hat{a}_{rr} + \hat{a}_{\varphi\varphi} + \hat{a}_{zz}.$$

It is worth noting that (36) has been obtained from (15), where the summand $\frac{1}{r}\frac{\partial}{\partial r}$ from the expression of $\Delta_{r,\varphi,z}$ was annihilated with a summand in the expression of $\frac{d^2\hat{Y}}{dr^2}$ written for new variable σ. The relations (27)–(37) should be supplemented with the conditions (see (20), (25)):

$$\begin{cases} \hat{w}\,|_{\sigma=0,1} = 0,\ \hat{Y}\,|_{\sigma=0} = 1,\ \hat{Y}\,|_{\sigma=1} = Y_H, \\ \hat{N}\,|_{\sigma=1} = \mathbb{C}_1 + \mathbb{C}_2 = \dfrac{n\hat{I}_H}{\hat{N}_0}\mu_H. \end{cases} \tag{38}$$

The dissipative functions Φ, Φ_m (see (18), (19)) computed on the vector-functions $\hat{\mathbf{U}}(r)$ (see (26)) are as follows:

$$\hat{\Phi} = \hat{a}_{rz}\frac{d\hat{w}}{dr}, \quad \hat{\Phi}_m = 0.$$

This has been used while deriving (36).

Note also that in (29) we can set $\hat{D} = 1$ by specific choosing the characteristic velocity u_H (see [4–7]).

We will assume for later use that the outer cylinder (it is denoted by the number '1' in the Figure 1) is made of the material with the electrical conductivity $\sigma_m = \sigma_m^1 = 0$, therefore in it $\Delta_{r,\varphi,z}N = 0$, i.e.

$$N = \hat{N}_1(r) = -\mathbb{C}_1^{(1)}\ln r + \mathbb{C}_2^{(1)},\ 1 < r < 1+h, \tag{39}$$

(39)

here in accordance with [21, 22] and (37)

$$\hat{N}_1(1) = \mathbb{C}_2^{(1)} = \mathbb{C}_2 = \frac{n\hat{I}_H}{\hat{N}_0}\mu_H - \mathbb{C}_1. \tag{40}$$

On the boundary $r = 1+h$ one gets

$$1 = -\mathbb{C}_1^{(1)}\ln(1+h) + \frac{n\hat{I}_H}{\hat{N}_0}\mu_H - \mathbb{C}_1. \tag{41}$$

Let us assume that the inner wall of the outer cylinder has *the absolute conductivity*, i.e. (see for instance [15,16]):

$$\left.\frac{\partial\hat{N}}{\partial\sigma}\right|_{\sigma=0} = \mathbb{C}_1 = 0. \tag{42}$$

From (41), (42) we obtain

$$\mathbb{C}_1^{(1)} = \left(-1 + \frac{n\hat{I}_H}{\hat{N}_0}\mu_H\right)/\ln(1+h)$$

and

$$\hat{N}_1(r) = \frac{n\hat{I}_H}{\hat{N}_0}\mu_H - \frac{\ln r}{\ln(1+h)}\left(\frac{n\hat{I}_H}{\hat{N}_0}\mu_H - 1\right),$$

$$1 < r < 1+h.$$

If the inner wall of the outer cylinder is *insulator*, see [15,16], we obtain

$$\hat{N}(0) = \mathbb{C}_2 = 0$$

and using (39)–(41) derive:

$$\mathbb{C}_1 = \frac{n\hat{I}_H}{\hat{N}_0}\mu_H, \quad \mathbb{C}_1^{(1)} = -\frac{1}{\ln(1+h)}$$

and

$$\hat{N}_1(r) = \frac{\ln r}{\ln(1+h)}, \quad \hat{N}(\sigma) = \frac{n\hat{I}_H}{\hat{N}_0}\mu_H\sigma.$$

A careful analysis of the relations (28)–(35) performed in [18] on the basis of [6] yields

$$\hat{a}_{\varphi\varphi} = \hat{a}_{\varphi z} = \hat{a}_{r\varphi} = 0,$$

i.e $\mathbb{C}_{r\varphi} = 0$ and for calculation of functions $\hat{a}_{rr}$, $\hat{a}_{zz}$, $\hat{w}$ we get the following relations (here the function $\hat{a}_{rz}$ can be obtained from (29)):

$$K_{\hat{I}}\hat{a}_{rr} + \beta\left(\hat{a}_{rr}^2 + \hat{g}\right) = 0,\ \hat{g} = \hat{a}_{rz}^2, \tag{43}$$

$$\hat{w}_\sigma = -\frac{\tilde{K}_{\hat{I}}\hat{Y}\hat{a}_{rz}}{J(\hat{Y})\hat{A}_r\hat{\nu}} = -\frac{\tilde{K}_{\hat{I}}}{J(\hat{Y})\hat{A}_r}\xi_0\tilde{Z}, \tag{44}$$

$$\tilde{K}_{\hat{I}} = K_{\hat{I}} + \beta\hat{I}.$$

Substituting this into (32) one obtains

$$K_{\hat{I}}\hat{a}_{zz} + \beta\,\|\,\hat{\vec{a}}_z\,\|^2 - 2\hat{g}\frac{\tilde{K}_{\hat{I}}}{\hat{A}_r} = 0. \tag{45}$$

Following [4,18] it is easy to obtain from (43), (45) the relations

$$\hat{a}_{zz} = \left(\hat{a}_{rr} + \frac{2\hat{g}}{\hat{A}_r}\right), \quad \hat{I} = 2\left(\hat{a}_{rr} + \frac{\hat{g}}{\hat{A}_r}\right).$$

Hereinafter we shall assume that $\overline{k} = 0$ ($k = \beta$). Thus, from (43) it follows that

$$\hat{a}_{rr} = \frac{-1 \pm \sqrt{1-\hat{G}}}{2\tilde{W}}, \ \hat{G} = 4\tilde{W}^2 \hat{g} \le 1, \qquad \tilde{W} = W\beta. \tag{46}$$

Later for definiteness we shall consider only the branch of the function $\hat{a}_{rr}$ with the '+' sign. Accounting for (38) from (44) one gets

$$\hat{w} = \xi_0 \left[-\mathfrak{F}_0(\sigma, \overline{\mathbb{C}})\overline{\mathbb{C}} + \mathfrak{F}_1(\sigma, \overline{\mathbb{C}}) \right], \tag{47}$$

where

$$\mathfrak{F}_0(\sigma, \overline{\mathbb{C}}) = \int_0^\sigma \mathfrak{F}(s, \overline{\mathbb{C}}) ds,$$

$$\mathfrak{F}_1(\sigma, \overline{\mathbb{C}}) = \int_0^\sigma \mathfrak{F}(s, \overline{\mathbb{C}}) \left[\tilde{D} e^{-2\xi_0 \sigma} - \mathrm{Ga}^* \xi_0 \int_0^\sigma e^{-2\xi_0 \lambda} \hat{Y} d\lambda \right] ds,$$

$$\mathfrak{F}(s, \overline{\mathbb{C}}) = \frac{\tilde{K}_{\hat{I}}(s)}{J(\hat{Y}(s))\hat{A}_r(s)} =$$

$$\exp\left(\overline{E}_A \frac{\hat{Y}(s)-1}{\hat{Y}(s)} \right) \frac{1 + 2\tilde{W}\left(\hat{a}_{rr}(s) + \hat{g}(s)/\hat{A}_r(s) \right)}{1 + W\hat{a}_{rr}(s)}.$$

Since $\hat{w}|_{\sigma=1} = 0$ (see (38)), then from (47) the relation for calculation of the constant $\overline{\mathbb{C}}$ follows:

$$\overline{\mathbb{C}} = \frac{\mathfrak{F}_1(1, \overline{\mathbb{C}})}{\mathfrak{F}_0(1, \overline{\mathbb{C}})}. \tag{48}$$

Making the following substitution into (36)

$$\hat{Y}(\sigma) = \hat{Q}(\sigma) + \hat{V}(\sigma), \ \hat{V}(\sigma) = 1 + (Y_H - 1)\sigma,$$

one can get the following boundary value problem

$$\hat{Q}_{\sigma\sigma} + A\xi_0^2 [\tilde{Z}(\hat{Q})]^2 \mathfrak{F}(\sigma, \overline{\mathbb{C}}, \hat{Q}) = 0, \qquad \hat{Q}(0) = \hat{Q}(1) = 0. \tag{49}$$

Here we have underlined the nonlinearity of differential equation for $\hat{Q}$ by denoting $\tilde{Z} = \tilde{Z}(\hat{Q})$ and $\mathfrak{F}(\sigma, \overline{\mathbb{C}}) = \mathfrak{F}(\sigma, \overline{\mathbb{C}}, \hat{Q})$.

A simple inspection reveals that the boundary value problem (49) has the strong singularity in the case of small values of radius of the inner cylinder r_0, see Figure 1. Indeed, since $\xi_0 = -\ln r_0$ and $\xi_0 \to \infty$ as $r_0 \to 0$, then the equation (49) can be regarded as one with the small parameter $1/\xi_0^2$ at the highest order derivative. The mentioned singularity cardinally effects not only the distribution of temperature, but also the distribution of the velocity of flow. For solving this problem we use special pseudospectral algorithm based on Chebyshev approximations. Its detailed description is given in [7,8]. To use it, it is convenient to drop "^" above "Q" and rewrite (49) as follows

$$Q_{\sigma\sigma} = -A\xi_0^2 [\tilde{Z}(Q)]^2 \mathfrak{F}(\sigma, \overline{\mathbb{C}}, Q) = f(\sigma, Q), \qquad Q(0) = Q(1) = 0. \tag{50}$$

4 Description of the pseudospectral numerical algorithm

In this section the fast pseudospectral algorithm is developed on the basis of Chebyshev approximations. The remarkable properties of such approximations and spectral methods based on them are described in vast literature (see [9,10,24] for instance). Below we detail the most important of them.

For solving the equation (50) we apply the iterative stabilization (or relaxation) technique. It requires to introduce a fictive time variable t that will be used for iterations and the regularizing operator (the regularization) B_t. Assuming that $Q = Q(\sigma, t)$ we shall seek the solution of (50) as the limit of solutions of the evolution equation

$$B_t Q = Q_{\sigma\sigma} - f(\sigma, Q)$$

as $t \to \infty$. In this work the Sobolev's regularization $B_t = \left(k_1 - k_2 \frac{\partial^2}{\partial \sigma^2} \right) \frac{\partial}{\partial t}$ is used, where $k_1, k_2 > 0$ are constants. By introducing the grid with respect to t with the step τ and the nodes $t_n = n\tau$, $n = 1, 2, \ldots$ and by denoting $Q^{[n]} = Q^{[n]}(\sigma) = Q(\sigma, t_n)$ we approximate the derivative Q_t by the difference quotient $(Q^{[n]} - Q^{[n-1]})/\tau$. Using the Sobolev's regularization of (50) we obtain:

$$k_1 Q^{[n]} - (k_2 + \tau) Q^{[n]}_{\sigma\sigma} = \left(k_1 - k_2 \frac{\partial^2}{\partial \sigma^2} \right) Q^{[n-1]} - \tau f(\sigma, Q^{[n-1]}) = \tilde{f}(\sigma, Q^{[n-1]}). \tag{51}$$

The idea of the method consists in finding the solution $Q^{[n]}$ to (51) on the current time step using its values $Q^{[n-1]}$ from the previous one. This

process should continue till the solution stabilized. More precisely, the stopping criteria is

$$\| B_t Q \| \le \varepsilon_S, \tag{52}$$

where ε_S is the error (or residual) of the stabilization process, $\|\cdot\|$ is the uniform norm of function (all the functions are assumed to be continuous).

In order to approximate in regularized equation (51) the values of $Q^{[n]}$ and the values of its derivatives with respect to σ, we use the modified interpolation polynomial with Chebyshev nodes written in the Lagrange form (see [11])

$$Q(\sigma) \approx p_N(Q,\sigma) = \\ = \sum_{j=1}^{N} \frac{s(\tilde\sigma,\sigma_j) T_N(\tilde\sigma)}{(\tilde\sigma-\sigma_j) T_N'(\sigma_j)} Q(\tilde\sigma_j), \tag{53}$$

$$\sigma_j = \cos\frac{2j-1}{2N}\pi$$

where $s(\tilde\sigma,\sigma_j) = \dfrac{1-\tilde\sigma^2}{1-\sigma_j^2}$,

$T_N(\tilde\sigma) = \cos(N \arccos\tilde\sigma), \tilde\sigma = 2\sigma - 1 \in [-1,1]$,

$\tilde\sigma_j = (\sigma_j + 1)/2$ and the dash means the differentiation with respect to σ.

We called this polynomial "modified" due to the factor $s(\tilde\sigma,\sigma_j)$ that was introduced to satisfy automatically the homogenous boundary conditions of (50).

For solving the equation (51) we use the (53) and the collocation method. The expansion (53) was differentiated with respect to σ. Further

$\vec{Q} = \vec{Q}^{[n]} = (Q(\tilde\sigma_1),...,Q(\tilde\sigma_N))^T$,

$\vec{Q}_\sigma = \vec{Q}_\sigma^{[n]} = (Q'(\tilde\sigma_1),...,Q'(\tilde\sigma_N))^T$,

$\vec{Q}_{\sigma\sigma} = \vec{Q}_{\sigma\sigma}^{[n]} = (Q''(\tilde\sigma_1),...,Q''(\tilde\sigma_N))^T$.

Here and in what follows the upper index "$[n]$" of the components of vectors $\vec{Q}$, $\vec{Q}_\sigma$, $\vec{Q}_{\sigma\sigma}$ and the arrows above vector notations are omitted.

$$p_N'(Q,\sigma) = H\sum_{j=1}^{N}(-1)^{j-1}Q_j \cdot \\ \left\{ \frac{2\tilde\sigma\sigma_j - \tilde\sigma^2 - 1}{N(\tilde\sigma-\sigma_j)^2\gamma_j} T_N(\tilde\sigma) + \right. \\ \left. + \frac{\gamma}{\gamma_j(\tilde\sigma-\sigma_j)} \sqrt{1-T_N^2(\tilde\sigma)} \right\}, \tag{54}$$

$$p''(Q,\sigma) = H^2\sum_{j=1}^{N}(-1)^{j-1}Q_j \cdot \\ \left\{ \frac{2\gamma_j^2 - N^2(\tilde\sigma-\sigma_j)^2}{N(\tilde\sigma-\sigma_j)^3\gamma_j} T_N(\tilde\sigma) - \right. \\ \left. - \frac{(\tilde\sigma^2 - 3\tilde\sigma\sigma_j + 2)}{\gamma\gamma_j(\tilde\sigma-\sigma_j)^2} \sqrt{1-T_N^2(\tilde\sigma)} \right\} \tag{55}$$

where $\gamma = \sqrt{1-\tilde\sigma^2}$, $\gamma_j = \sqrt{1-\sigma_j^2}$, $H = \sqrt{2}$. The limit expressions of the first and second derivatives (54), (55) as $\sigma \to \tilde\sigma_i$ were obtained using l'Hospital's rule.

$$p_N'(Q,\sigma_i) = H\left(\sum_{\substack{j=1,\\ j\ne i}}^{N} (-1)^{i+j} \frac{\gamma_i}{\gamma_j(\sigma_i-\sigma_j)} Q_j - \frac{3\sigma_i}{2\gamma_i^2} Q_i \right),$$

$$p_N''(Q,\sigma_i) = H^2\left(\sum_{\substack{j=1,\\ j\ne i}}^{N} (-1)^{i+j-1} \frac{2\gamma_i^2 + 3\sigma_i(\sigma_i-\sigma_j)}{\gamma_j\gamma_i(\sigma_i-\sigma_j)^2} Q_j - \right. \\ \left. - \frac{(N^2+5)\gamma_i^2 + 3\sigma_i^2}{3\gamma_i^4} Q_i \right)$$

Let us denote

$$\mathfrak{a}_{ij} = \frac{(-1)^{i+j}\gamma_i}{\gamma_j(\sigma_i-\sigma_j)}, \quad a_{ij} = (-1)^{i+j-1}\frac{2\gamma_i^2 + 3\sigma_i(\sigma_i-\sigma_j)}{\gamma_j\gamma_i(\sigma_i-\sigma_j)^2}, \\ i,j = 1,...,N, i \ne j,$$

$$\mathfrak{n}_i = -3\sigma_i/(2\gamma_i^2), \quad \nu_i = -((N^2+5)\gamma_i^2 + 3\sigma_i^2)/(3\gamma_i^4), \\ i = 1,...,N$$

and make up $N \times N$ matrices

$$\mathfrak{A} = H \begin{pmatrix} \mathfrak{n}_1 & \mathfrak{a}_{12} & \dots & \mathfrak{a}_{1N} \\ \mathfrak{a}_{21} & \mathfrak{n}_2 & \dots & \mathfrak{a}_{2N} \\ \vdots & \vdots & \dots & \vdots \\ \mathfrak{a}_{N1} & \mathfrak{a}_{N2} & \dots & \mathfrak{n}_N \end{pmatrix}, \quad A = H^2 \begin{pmatrix} \nu_1 & a_{12} & \dots & a_{1N} \\ a_{21} & \nu_2 & \dots & a_{2N} \\ \vdots & \vdots & \dots & \vdots \\ a_{N1} & a_{N2} & \dots & \nu_N \end{pmatrix}. \tag{56}$$

Then we come to the matrix approximation of the derivatives:

$$\vec{Q}_\sigma \approx \mathfrak{A}\vec{Q}, \quad \vec{Q}_{\sigma\sigma} \approx A\vec{Q}, \tag{57}$$

The spectral decomposition of matrix A approximating the second-order derivative was used to construct the numerical algorithm

$$A = R_A D_A R_A^{-1},$$

where R_A is the matrix of eigenvectors of A; D_A is the diagonal matrix containing the eigenvalues d_A^j of A, $j = 1,...,N$. Strictly speaking, in the case when A has complex-conjugate eigenvalues, the matrix D_A is block diagonal matrix containing the 2×2-blocks on the diagonal. But in our numerical tests this situation was not observed. An important property of the method is also the slow growth of the condition number of matrix R_A and of the norms of matrices $\mathfrak{A}$, A with the growth of N. This provides high numerical stability of the algorithm.

Using (53) for solving (51) by collocation method one obtains a system of linear equations with the matrix $k_1 E - (k_2 + \tau)A$ (E is the identity matrix). Multiplying the system by the matrix R_A^{-1} from the left one gets

$$k_1 V^{[n]} - (k_2 + \tau) D_A V^{[n]} = G^{[n]}, \tag{58}$$

where $V^{[n]} = R_A^{-1}\vec{Q}^{[n]}$, $G^{[n]} = R_A^{-1}\tilde{F}(\vec{Q}^{[n-1]})$ are the vectors of size N, $\tilde{F} = \tilde{F}(\vec{Q}^{[n-1]})$ is the vector of values of $\tilde{f}(\sigma, \vec{Q}^{[n-1]})$ in the collocation nodes $\tilde{\sigma}_j$, $j = 1,...,N$. Now we are able to find the components of the vector $V^{[n]}$ using the values of components g_j of the vector $G^{[n]}$:

$$v_j = \frac{g_j}{k_1 - (k_2 + \tau) d_A^j}, \; j = 1,...,N. \tag{59}$$

As a result, the values of solution on the nth time step have been obtained: $\vec{Q}^{[n]} = R_A V^{[n]}$. From (59) it follows that the conditions necessary for convergence of the proposed method are $\tau \neq k_1 / d_A^j - k_2$, $\forall j$.

Note that the number of operations required for computing the solution on each time step is defined by the products of matrices and vectors, namely $G^{[n]} = R_A^{-1}\tilde{F}(\vec{Q}^{[n-1]})$ and $\vec{Q}^{[n]} = R_A V^{[n]}$. This number is $2N^2$ by the order of the magnitude of N.

The described algorithm enables us to obtain the approximate solution of the problem (51) on the current nth time step of the stabilization method. Below the upper index "$[n]$" at all of the variables means the number of time step. In order to pass to the next time step the following procedures should be done allowing also to calculate the values velocity $\hat{w}$ in the points $\tilde{\sigma}_j$, $j = 1,...,N$.

• Compute $\hat{g}^{[n+1]}(\tilde{\sigma}_j)$ as in (43) by expressing $\hat{a}_{rz}^{[n+1]}(\tilde{\sigma}_j)$ from (29) and by using the value $\hat{Y}^{[n]}(\tilde{\sigma}_j) = \hat{Q}^{[n]}(\tilde{\sigma}_j) + \hat{V}(\tilde{\sigma}_j)$ computed on the current time step.

• Calculate $\hat{G}^{[n+1]}(\tilde{\sigma}_j)$ and $\hat{a}_{rr}^{[n+1]}(\tilde{\sigma}_j)$ by (46) and $\hat{A}_{rr}^{[n+1]}(\tilde{\sigma}_j) = \hat{a}_{rr}^{[n+1]}(\tilde{\sigma}_j) + W^{-1}$.

• Compute the values of integrals $\mathfrak{F}_0^{[n+1]}(\tilde{\sigma}_j, \overline{\mathbb{C}}^{[n]})$, $\mathfrak{F}_1^{[n+1]}(\tilde{\sigma}_j, \overline{\mathbb{C}}^{[n]})$ with variable upper limits $\tilde{\sigma}_j$ using known values of $\hat{g}^{[n+1]}(\tilde{\sigma}_j)$, $\hat{a}_{rr}^{[n+1]}(\tilde{\sigma}_j)$, $\hat{A}_r^{[n+1]}(\tilde{\sigma}_j)$, $\hat{Y}^{[n]}(\tilde{\sigma}_j)$ and $\overline{\mathbb{C}}^{[n]}$.

• Using (47) and (48) obtain the values of velocity of flow $\hat{w}^{[n+1]}(\tilde{\sigma}_j)$ and the constant value of $\overline{\mathbb{C}}^{[n+1]}$.

• Using (29) compute the values of $\tilde{Z}^{[n+1]}(\tilde{\sigma}_j)$.

• Finally, compute the right hand side $f(\tilde{\sigma}_j, \vec{Q}^{[n]})$ of (50) on the next $(n+1)$th time step.

Using the described procedures we can pass from step to step until the solution stabilized. Since there is no general theory proving that such stabilization process converges (but some useful comments for the case of linear problems can be found for example in [25]), we have performed the multiparametric numerical simulation and found the sets of physical parameters allowing to obtain this convergence, and hence to get the sought-for stationary solution of (50). During this investigation we also got the appropriate values of stabilization

parameters k_1, k_2, τ that enables us to decrease the number of time steps in dozens and hundreds of times while simulating the regimes with the record-low values of r_0.

It is worth noting, that for computing the integral expressions in our algorithm we used the fast Fourier transform for the values of the integrand in the points of Chebyshev grid. This reduces the number of operations required for computing the right hand side of (50) from $O(N^2)$ operations to $O(N \ln N)$.

5 Numerical simulations of magnetohydrodynamic flows with the heat dissipation

The described algorithm was implemented in Matlab. The program has been run on the computer Intel Core i5-3330, 3.00 GHz, 8 Gb DIMM DDR3 RAM. The stationary regimes of non-isothermal magnetohydrodynamic flow of polymeric fluid have been simulated taking into account the heat dissipation effect and the electromagnetic impact. Note, that the values of phenomenological parameter β, of heat dissipation constant A and of energy of activation E_A should be set based on the results of the mechanical tests, while the value of magnetic susceptibility has been taken from reference tables. Under assumption that heating element is made of tungsten we took $\chi_{OH} = 7.8 \cdot 10^{-5}$. For definiteness we fix $\beta = 0.1$, $E_A = 9$. The investigation of the impact of heat dissipation has been done by varying A. The investigation of electromagnetic impact has been done by varying the parameters a, b in (24) that in our model influence only Y_H.

Let us compute the solutions $\hat{w}$ and $\hat{Y}$, using the described algorithm and find their dependance on parameters r_0, $\hat{D}$, W, A, a, b (see Table 1 and Figures 3–8).

Table 1. Parameters of simulated regimes.

No. of test	No. of figure	r_0	$\hat{D}$	W	A	Y_H
1	Fig. 3	0.2–0.0002	1	–1	0.01	3
2	Fig. 4	0.001	0–10	–1	0.01	7/3
3	Fig. 5	0.01	1	–1–0.8	0.01	1
4	Fig. 6	0.01	5	–1	0.01–6	2
5	Fig. 7	0.2	2	–1	0.01	1/10—9/10
6	Fig. 8	0.2	2	–1	0.01	1/3—3

The interesting effect appears in Figure 3. With the decrease in radius of the heating element r_0 the velocity profile changes qualitatively. The smaller the radius is, the smaller the area of the surface of heating element is, and so does the heat transfer. Near the heating element the convective flow can be observed, but while the radius decreases the upward convective flow becomes smaller and smaller due to reduction of the heat transfer. When the radius reaches the threshold value of $r_0 \approx 0.04$ the flow of liquid in the neighborhood of the inner cylinder becomes oriented downward.

With the growth of dissipation constant A, the modulus of velocity grows essentially. The graph of temperature, as expected, becomes more symmetric (see Figure 4).

The characteristic of pressure gradient and of viscosity $\hat{D}$ and Weissenberg number W influences the velocity essentially, but almost do not affect the distribution of temperature in liquid. It can be observed in Figures 5, 6. The velocity profiles are directed downwards for $\hat{D} < 0$ and upwards for $\hat{D} > 0$.

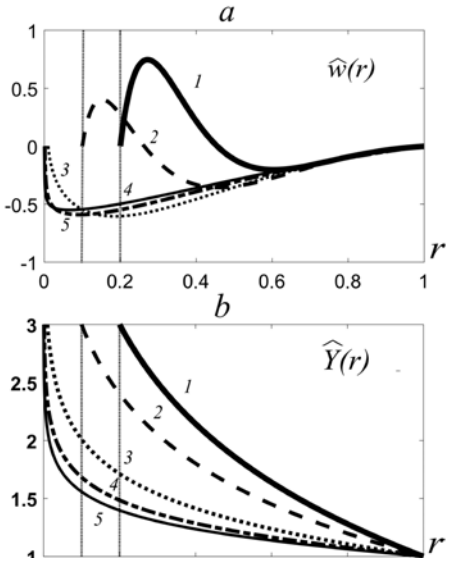

Fig.3. Distributions of velocity of liquid (a) and of temperature (b) obtained in numerical simulations with $\beta = 0.1$, $\hat{D} = -1$, $E_A = 9$, $W = 0.01$, $A = 1$, $Y_H = 3$ for different values of r_0 ($r_0 = 0.2$ in the test No. 1, $r_0 = 0.1$ in test No. 2, $r_0 = 0.01$ in test No. 3, $r_0 = 0.001$ in test No. 4, $r_0 = 0.0002$ in test No. 5).

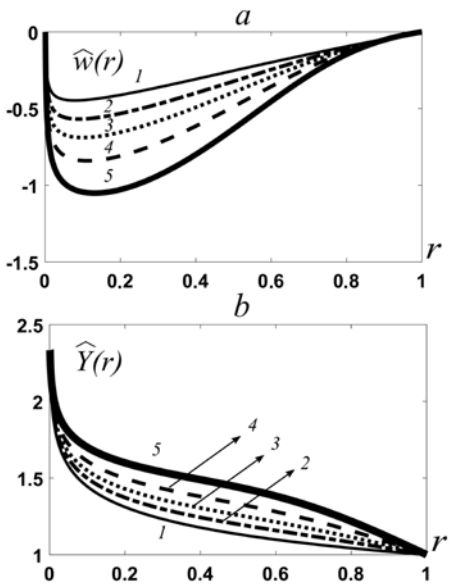

Fig.4. Distributions of velocity of liquid (a) and of temperature (b) obtained in numerical simulations with $r_0 = 0.001$, $\beta = 0.1$, $\hat{D} = -1$, $E_A = 9$, $W = 0.01$, $Y_H = 7/3$ for different values of A ($A = 0$ in the test No. 1, $A = 2$ in test No. 2, $A = 5$ in test No. 3, $A = 7$ in test No. 4, $A = 10$ in test No. 5).

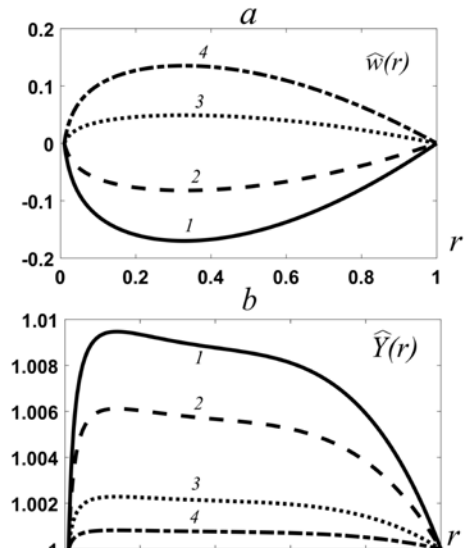

Fig.5. Distributions of velocity of liquid (a) and of temperature (b) obtained in numerical simulations with $r_0 = 0.01$, $\beta = 0.1$, $E_A = 9$, $W = 0.01$, $A = 1$, $Y_H = 1$ for different values of $\hat{D}$ ($\hat{D} = -1$ in the test No. 1, $\hat{D} = -0.5$ in test No. 2, $\hat{D} = 0.3$ in test No. 3, $\hat{D} = 0.8$ in test No. 4).

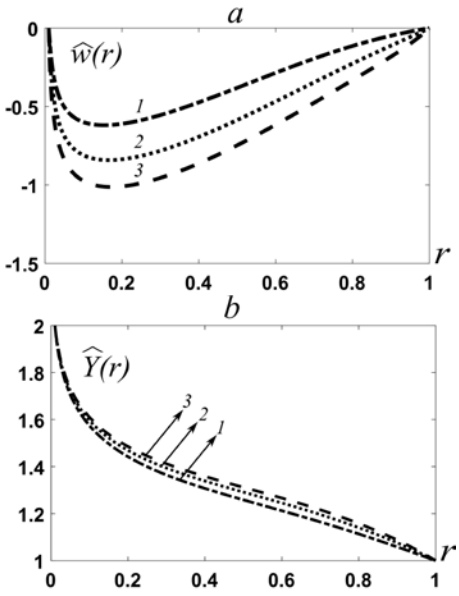

Fig.6. Distributions of velocity of liquid (a) and of temperature (b) obtained in numerical simulations with $r_0 = 0.01$, $\beta = 0.1$, $E_A = 9$, $\hat{D} = -1$, $A = 5$, $Y_H = 2$ for different values of W ($W = 0.01$ in the test No. 1, $W = 5$ in test No. 2, $W = 6$ in test No. 3).

Let us recall that in (24) we introduce the parameters $a = \frac{n\hat{I}_H}{\hat{N}_0}$ and $b = \frac{\widehat{\mathfrak{m}}_H}{\hat{N}_0}$. In Figures 7 and 8 the dependence of the solution on these parameters is shown. In Figure 8 the effect associated with convection in the gravitational field is also obvious. Starting from $a \approx 7.4$ ($Y_H \approx 2.4$) the velocity profile takes positive values. The thermal energy (which is quite large near the heating element) is converting into the kinetic one of the fluid flow directed against gravity. Therefore, for sufficiently large values of a and/or for small values of b.

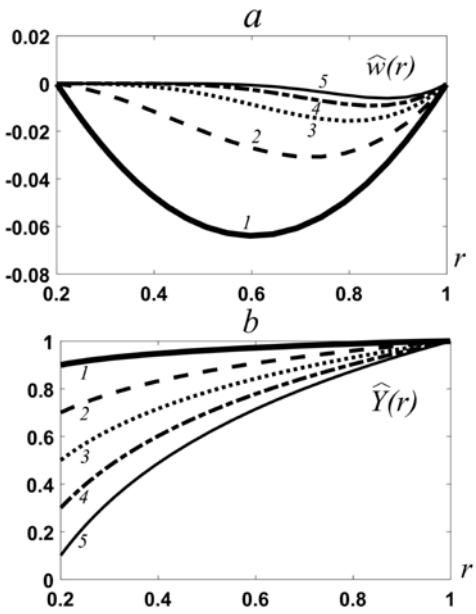

Fig.7. Distributions of velocity of liquid (a) and of temperature (b) obtained in numerical simulations with $r_0 = 0.2$, $\beta = 0.1$, $E_A = 9, \hat{D} = -1, A = 2$, $b = 10$ for different values of a (a = 9 in the test No. 1, a = 7 in test No. 2, a = 5 in test No. 3, a = 3 in test No. 4, a = 1 in test No. 5).

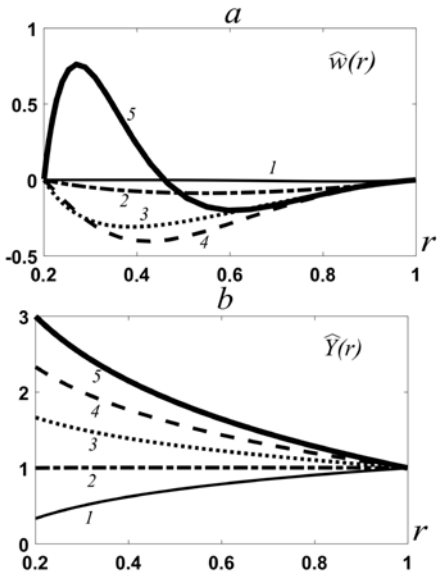

Fig.8. Distributions of velocity of liquid (a) and of temperature (b) obtained in numerical simulations with $r_0 = 0.2$, $\beta = 0.1$, $E_A = 9, \hat{D} = -1$, $A = 2$, $b = 3$ for different values of a (a = 9 in the test No. 1, a = 7 in test No. 2, a = 5 in test No. 3, a = 3 in test No. 4, a = 1 in test No. 5).

Now let us a bit focus on the performance of the desired algorithm and the choice of numerical parameters. In this connection we consider the regimes with $\beta = 0.3$, $\hat{D} = 1$, $E_A = 1$, $W = 0.01$, $\bar{\theta} = 2$, Ga=1 and vary of r_0 starting from r_0=0.5 up to r_0=0.001 (as $A = 1$) and also vary the dissipation constant A starting from $A = 0$ up to $A = 12$ (as $r_0 = 0.001$). All of these tests have been done with the numerical parameters $k_1 = k_2 = 1$, $N = 101$.

Table 2 contains the parameters of the computational process for the mentioned tests, they are the time step τ of iteration process, the stabilization residual ε_S, the number of iterations N_{it}, the run times of algorithm t_A in milliseconds, the maximum value M of the velocity $w(r)$ and the coordinate r_M of this maximum.

Table 2. Numerical parameters used in simulations with $\beta = 0.3$, $\hat{D} = 1$, $E_A = 1$, $W = 0.01$, $\overline{\theta} = 2$ ($\mathrm{Ga}^* = 1$), $N = 101$.

Regime	τ	ε_S	N_{it}	t_A (ms)	M	r_M
$A = 0$	1	3.3E-10	9	44	0.2771	0.2039
$A = 3$	1000	8.4E-11	13	96	0.2988	0.2063
$A = 6$	10^6	5.5E-11	13	75	0.3287	0.2093
$A = 9$	10^6	9.3E-11	20	142	0.3761	0.2133
$A = 12$	10^6	1.4E-10	61	334	0.4987	0.2204
$r_0 = 0.5$	1000	1.4E-11	6	31	0.0895	0.7071
$r_0 = 0.1$	1000	6E-11	8	49	0.2523	0.3861
$r_0 = 0.01$	10^6	5.2E-11	6	32	0.2853	0.2555
$r_0 = 0.001$	10^6	5.4E-12	7	44	0.2837	0.2046

6 Conclusion

In this work, the mesoscopic rheological Pokrovsky–Vinogradov model has been used for constructing a new model of the non-isothermal magnetohydrodynamical flow of incompressible polymeric liquid between two coaxial cylinders. This model has been simplified for simulating the flow similar to Poissel's one and tested numerically for a wide range of physical parameters. In our tests we have focused on searching the ways of manipulating the flows of polymeric liquid by different impacts that is of a high importance for additive manufacturing industry. Another goal was to reduce of the time and memory consumptions while computing the regimes with extremely small values of the radius of the inner cylinder. To this end we used the pseudospectral algorithm without saturation based on Chebyshev approximations and the stabilization time-stepping technique.

One can observe from the graphs that the influence of the heat dissipation term is significant. When A grows, the temperature distribution tends to become symmetric and the values of velocity grow essentially. It is well known that for non-isothermal flows of Newton liquids described by Navier–Stokes equations the contribution of heat dissipation is very essential for physically reliable modelling. We can assume with the high rate of confidence that the same is valid for the flows of polymeric liquids especially for applications in the technology of thermal inkjet printing working with the thing heating elements in printheads, where the gradients of temperature and the velocity of flow can be extremely steep.

Electromagnetic impact changes the considered flow cardinally. By varying the electrical strength, magnetic field intensity and the winding of the inner cylinder one can manipulate the flow changing its main characteristics both quantitatively and qualitatively for getting the desired parameters of technological process of 3D printing.

References

1. Pokrovskii, V.N.: *The Mesoscopic Theory of Polymer Dynamics*. 2nd edn. Springer, Berlin (2010), 256 pp.

2. Vinogradov, G. V., Pokrovskii, V. N., Yanovsky, Yu. G.: Theory of Viscoelastic Behavior of Concentrated Polymer Solutions and Melts in One-Molecular Approximation and its Experimental Verification. *Rheol. Acta* 7, 258–274 (1972)

3. Pyshnograi, G.V., Gusev, A. S. Pokrovskii, V.N.: Constitutive equations for weakly entangled

linear polymers. *Journal of Non-Newtonian Fluid Mechanics* 164(1–3), 17–28 (2009)

4. Blokhin, A. M., Rudametova, A. S.: Stationary solutions of the equations for nonisothermal electroconvection of a weakly conducting incompressible polymeric liquid. *Journal of Applied and Industrial Mathematics* 9(2), 147–156 (2015)

5. Blokhin, A. M., Semisalov, B. V.: A stationary flow of an incompressible viscoelastic fluid in a channel with elliptic cross section. *Journal of Applied and Industrial Mathematics* 9(1), 18–26 (2015)

6. Blokhin, A. M., Semisalov, B. V., Shevchenko, A.S.: Stationary solutions of equations describing the nonisothermal flow of an incompressible viscoelastic polymeric fluid. *Math. Modeling* 28(10), 3–22 (2016) (in Russian)

7. Blokhin, A.M., Kruglova, E.A., Semisalov, B.V.: Steady-state flow of an incompressible viscoelastic polymer fluid between two coaxial cylinders. *Computational Mathematics and Mathematical Physics* 57(7), 1181–1193 (2017)

8. Semisalov, B. V.: A fast nonlocal algorithm for solving Neumann–Dirichlet boundary value problems with error control. *Vychisl. Metody Programm*. 17(4), 500—522 (2016) (in Russian)

9. Achieser, N. I.: *Theory of Approximation*. Frederick Ungar Publishing Co, New York (1956), 307 pp.

10. Canuto, C., Hussaini, M. Y., Quarteroni, A., Zang, Th. A.: *Spectral Methods: Fundamentals in Single Domains*. Springer, Berlin Heidelberg (2006), 565 pp.

11. Babenko, K. I.: *Fundamentals of numerical analysis*. Moscow, Fizmatlit (1986) (in Russian), 744 pp.

12. Blokhin, A.M., Kruglova, E.A., Semisalov, B.V.: Numerical analysis of the non-isothermal flow of polymeric liquid between two coaxial cylinders. *WSEAS Transactions on Fluid Mechanics* 13, 26–36. Art.#4 (2018).

13. Altukhov, Yu.A., Gusev, A.S., Pyshnograi, G.V.: *Introduction to the Mesoscopic Theory of Flowing Polymer Systems*. Altai State Pedagogical Academy Press, Barnaul, (2012) (in Russian), 121 pp.

14. Sedov, L. I.: *Mechanics Of Continuous Media*. World Scientific (1997), 1368 pp.

15. Loitsyanskii, L. G., Stewartson, K.: *Mechanics of Liquids and Gases*. Stewartson Pergamon Press, Oxford (1966), 814 pp.

16. Vatazhin, A. B., Lubimov, G. A., Regirer, S. A.: *Magneto-Gas Dynamic Flows in Channels*. Nauka, Moscow (1970) (in Russian), 672 pp.

17. Shih-I, Pai: *Introduction to the Theory of Compressible Flow*. Literary Licensing, LLC (2013), 400 pp.

18. Blokhin, A. M., Rudametova, A. S.: Stationary flows of a weakly conducting incompressible polymeric liquid between coaxial cylinders. *Journal of Applied and Industrial Mathematics* 11(4), 486–493 (2017)

19. Shibata, Y.: On the *R*-Boundness for the Two Phase Problem with Phase Transitions: Compressiable–Incompressiable. Model Problem. *Funkcialaj Ekvacioj* 59, 243–287 (2016).

20. Nordling. C., Osterman, J.: *Physics Handbook for Science and Engineering*, 8th edn. Studentlitteratur AB (2006), 504 pp.

21. Achieser, A. I., Achieser, I. A. *Electromagnetism and electromagnetic waves*. High school publ., Moscow (1985) (in Russian), 504 pp.

22. Kalashnikov, S.G.: *Electricity. Science*, Moscow (1964) (in Russian)

23. Kubo, R.: *Thermodynamics. An Advanced Course with Problems and Solutions*. North Holland Publishing Company, Amsterdam 72(9–10) (1968)

24. Trefethen, L. N.: *Approximation Theory and Approximation Practice*. SIAM (2013), 295 pp.

25. Belov, A. A., Kalitkin, N. N.: Evolutionary factorization and superfast relaxation count. *Mathematical Models and Computer Simulations* 7(2), 103–116 (2015).